The Astronomical Journal, 135:1–9, 2008 January doi:10.1088/0004-6256/135/1/1

WHITE DWARF LUMINOSITY AND MASS FUNCTIONS FROM SLOAN DIGITAL SKY SURVEY SPECTRA

Steven DeGennaro[1], Ted von Hippel[1], D. E. Winget[1], S. O. Kepler[2], Atsuko Nitta[3], Detlev Koester[4], and Leandro Althaus[5,6]
[1] Department of Astronomy, The University of Texas at Austin, 1 University Station C1400, Austin, TX 78712-0259, USA
[2] Instituto de Física, Universidade Federal do Rio Grande do Sul, 91501-900 Porto-Alegre, RS, Brazil
[3] Gemini Observatory, Hilo, HI 96720, USA
[4] Institut für Theoretische Physik und Astrophysik, Universität Kiel, 24098 Kiel, Germany
[5] Facultad de Ciencias Astronómicas y Geofísicas, Universidad Nacional de La Plata, Paseo del Bosque S/N, 1900 La Plata, Argentina
[6] Instituto de Astrofísica La Plata, IALP, CONICET, Argentina
Received 2007 April 30; accepted 2007 September 13; published 2007 November 29

ABSTRACT

We present the first phase in our ongoing work to use Sloan Digital Sky Survey (SDSS) data to create separate white dwarf (WD) luminosity functions (LFs) for two or more different mass ranges. In this paper, we determine the completeness of the SDSS spectroscopic WD sample by comparing a proper-motion selected sample of WDs from SDSS imaging data with a large catalog of spectroscopically determined WDs. We derive a selection probability as a function of a single color ($g - i$) and apparent magnitude (g) that covers the range $-1.0 < g - i < 0.2$ and $15 < g < 19.5$. We address the observed upturn in log g for WDs with $T_{\rm eff} \lesssim 12{,}000$ K and offer arguments that the problem is limited to the line profiles and is not present in the continuum. We offer an empirical method of removing the upturn, recovering a reasonable mass function for WDs with $T_{\rm eff} < 12{,}000$ K. Finally, we present a WD LF with nearly an order of magnitude (3358) more spectroscopically confirmed WDs than any previous work.

Key words: stars: luminosity function, mass function – white dwarfs

Online-only material: color figures

1. INTRODUCTION

Since white dwarfs (WDs) cannot replenish the energy they radiate away—any residual nuclear burning is negligible and gravitational contraction is severely impeded by electron degeneracy—their luminosity decreases monotonically with time. A thorough knowledge of the rate at which WDs cool can provide a valuable "cosmic clock" to determine the ages of many Galactic populations, including the disk (Winget et al. 1987; Liebert et al. 1988; Leggett et al. 1998; Knox et al. 1999), and open and globular clusters (Claver 1995; von Hippel et al. 1995, 2006; Richer et al. 1998; Claver et al. 2001; Hansen et al. 2002, 2004, 2007; Jeffery et al. 2007). With more accurate models of the cooling physics of WDs, heavily constrained by empirical evidence, it may be possible to determine absolute ages with greater precision than using main-sequence evolution theory. In addition to applications in astronomy, WDs allow us to probe the physics of degenerate matter at temperatures and densities no terrestrial laboratory can duplicate.

Attempts at an empirical luminosity function (LF) for WDs date as far back as Luyten (1958) and Weidemann (1967). The low-luminosity shortfall, discovered by Liebert et al. (1979), and attributed by Winget et al. (1987) to the finite age of the Galactic disk, was confirmed and explored more fully when a greater volume of reliable data on low-luminosity WDs became available (Liebert et al. 1988; Wood 1992). More recently, Sloan Digital Sky Survey (SDSS) photometric data have been used to provide a much more detailed LF with more than an order of magnitude more WDs than previously attempted (Harris et al. 2006), as well a new LF of a large sample of spectroscopically confirmed WDs (Hu et al. 2007). However, to date no one has published a well-populated LF that does not include a wide range of masses and spectral types. Thus, much of the important physics of WD cooling remains buried in the data.

Until recently, empirical WD LFs, especially those derived from stars with spectra, have been hampered by a limited volume of reliable data. This has forced a trade-off between the number of stars included in a sample and their homogeneity; either a broad range of temperatures, masses, and spectral types must be used, or else the sample population of stars would be so small as to render reliable conclusions difficult. Recently, the situation has changed dramatically. Data from SDSS DR4 have yielded nearly 10,000 WD spectra. All of these spectra have been fitted with model atmospheres to determine their effective temperatures and surface gravities (Kleinman et al. 2004; Krzesiński et al. 2004; Eisenstein et al. 2006; Hügelmeyer et al. 2006; Kepler et al. 2007).

In a companion paper to be published shortly, we intend to focus on how the WD cooling rate changes with WD mass. Theoretical work has been done in this area (Wood 1992; Fontaine et al. 2001) but, to date, attempts at creating an empirical LF to explore the effects of mass have relied on limited sample sizes (Liebert et al. 2005). In order to further isolate the effect of mass, we have chosen to study only the DA WDs—those that show only lines of hydrogen in their spectra—which comprise ~86% of all WDs.

In addition to helping unlock the physics of WDs, creating LFs for several mass bins can also help to disentangle the effects of changes in cooling rates from changes in star formation rates. A burst or dip in star formation at a given instant in Galactic history should be recorded in all of the LFs, regardless of mass, and could be confirmed by its position across the various mass bins. For example, a short burst of increased star formation would be seen as a bump in each LF, occurring at cooler temperatures in the higher mass LF (these stars, with shorter main sequence (MS) lifetimes, have had longer to cool). On the other hand, features intrinsic to the cooling physics of the WDs themselves should be seen in places that correspond with the underlying physics, which may be earlier,

later, or nearly concurrent across mass bins. These effects include neutrino cooling, crystallization, the onset of convective coupling (Fontaine et al. 2001), and Debye cooling (Althaus et al. 2007).

The current paper lays the groundwork for this analysis. In Section 2, we introduce the data, examining the methods used to classify spectra and derive quantities of interest (dominant atmospheric element, $T_{\rm eff}$, and log g). We also address the observed upturn in log g for DAs below $T_{\rm eff} \sim 12{,}000$ K. We present several lines of reasoning that the upturn is an artifact of the line-fitting procedure, and propose an empirical method for correcting the problem. Section 3 outlines the methods used to construct the luminosity and mass function and determine error bars.

In Section 4, we present an analysis of the completeness of our data sample. We use a well-defined sample of proper-motion selected, photometrically determined WDs in the SDSS (Harris et al. 2006) to determine our completeness and derive a correction as a function of $g-i$ color and g magnitude. Finally, in Section 5, we present our best luminosity and mass functions for the entire DA spectroscopic sample and discuss the impact of both our empirical log g correction and our completeness correction.

Table 1
The Fraction of Stars in Eisenstein et al. (2006)

$M_{\rm bol}$	DA Fraction
7.25	0.9338
7.75	0.9243
8.25	0.9246
8.75	0.8980
9.25	0.8433
9.75	0.8146
10.25	0.7958
10.75	0.8158
11.25	0.7957
11.75	0.7721
12.25	0.7985
12.75	0.7976
13.25	0.8173
13.75	0.8009

Notes. Listed as DA or DA_auto. Though the values generally agree with previous results, they should be used with much caution, as they were calculated crudely and we have taken no care to correct for biases in the sample. We have employed them here simply to compare our DA-only LF to previous work.

2. THE DATA

Our WD data come mainly from Eisenstein et al. (2006), a catalog of spectroscopically identified WDs from the Fourth Data Release (DR4) of the Sloan Digital Sky Survey (York et al. 2000). The SDSS is a survey of ∼8000 square degrees of sky at high Galactic latitudes. It is, first and foremost, a redshift survey of galaxies and quasars. Large "stripes" of sky are imaged in five bands (u, g, r, i, and z) and objects are selected, on the basis of color and morphology, to be followed up with spectroscopy, accomplished by means of twin fiber-fed spectrographs, each with separate red and blue channels with a combined wavelength coverage of about 3800 to 9200 Å and a resolution of 1800 Å. Objects are assigned fibers based on their priority in accomplishing SDSS science objectives, with high redshift galaxies, "bright red galaxies", and quasars receiving the highest priority. Stars are assigned fibers for spectrophotometric calibration, and other classes of objects are only assigned fibers that are left over on each plate. More detailed descriptions of the target selection and tiling algorithms can be found in Stoughton et al. (2002) and Blanton et al. (2003).

Though WDs are given their own (low priority) category in the spectroscopic selection algorithms, very few WDs are targeted in this way. Rather, most of the WDs in the SDSS obtain spectra only through the "back door," most often when the imaging pipeline mistakes them for quasars. Kleinman et al. (2004) list the various algorithms that target objects ultimately determined to be WDs in Data Release 1 (DR1) (their Table 1). WDs are most commonly targeted by the QSO and SERENDIPITY_BLUE algorithms, with significant contributions also from HOT_STANDARD (standard stars targeted for spectrophotometric calibration) and SERENDIPITY_DISTANT. Of the significant contributors, the STAR_WHITE_DWARF category contributes the least to the population of WD spectra.

The SDSS Data Release 4 contains nearly 850,000 spectra. Several groups have already attempted to sort through them to find WDs: Harris et al. (2003) for the Early Data Release, Kleinman et al. (2004) for DR1, and most recently, Eisenstein et al. (2006) for the DR4, from which the majority of our data sample derives, though a handful of stars from DR1 omitted by Eisenstein have been reincluded from Kleinman et al. (2004). Most recently, Kepler et al. (2007) have refitted the DA and DB stars from Eisenstein et al. (2006) with an expanded grid of models. A complete analysis of the methods by which candidate objects are chosen, spectra fitted, and quantities of interest are calculated can be found in Kleinman et al. (2004), Eisenstein et al. (2006), and Kepler et al. (2007). We put forth a brief outline here, with special attention paid to those aspects important to our own analysis.

Objects in the SDSS spectroscopic database are put through several cuts in color designed to separate the WDs from the main stellar locus. Figure 1 in Eisenstein et al. (2006) shows the location of these cuts. The chief failing of their particular choices of cuts, as noted by the authors, is that WDs with temperatures below ∼8000 K begin to overlap in color–color space with the far more numerous A and F stars, and they have not attempted to dig these stars out. The SDSS spectroscopic pipeline calculates a redshift for each object by looking for prominent lines in the spectrum. Objects with redshifts higher than $z = 0.003$ are eliminated, unless the object has a proper motion from USNO-A greater than $0.3''$ year^{-1}. Since the spectroscopic pipeline is fully automated, occasionally DC WDs show weak noise features that can be misinterpreted as low-confidence redshifts. Other types of WDs, particularly magnetic WDs, can fool the pipeline as well. In the present paper, we are concerned chiefly with DA WDs, so this incompleteness is of importance only insofar as we use the entire set of WD spectral types to derive our completeness correction, as outlined in Section 4. We explore the implications of this more fully in that section.

Eisenstein et al. (2006) then use a χ^2-minimization technique to fit the spectra and photometry of the candidate objects with separate model atmospheres of pure hydrogen and pure helium (Finley et al. 1997; Koester et al. 2001) to determine the dominant element, effective temperature, surface gravity,

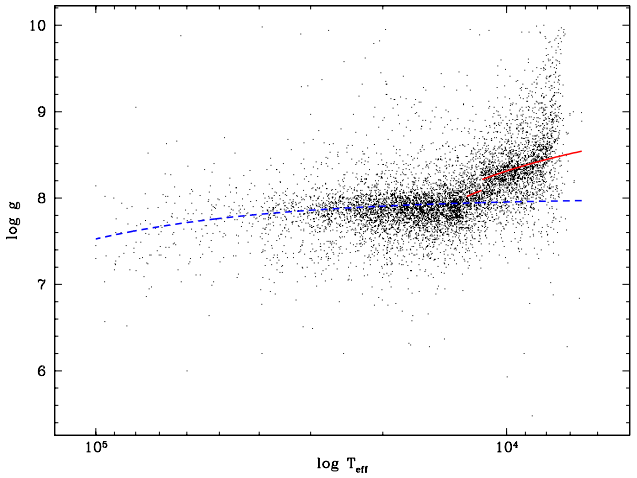

Figure 1. Plot of log g versus log $T_{\rm eff}$ for the WDs in our sample. At temperatures below ∼12,500 K, the log g values begin to rise to an extent unexplained by current theory. The solid line is a function empirically fit to the real data. The dashed line is the modest rise predicted by theory. The excess at a given $T_{\rm eff}$ is subtracted from the measured log g value for some of our LFs.

(A color version of this figure is available in the online journal)

and associated errors. As their Figure 2 demonstrates, they recover a remarkably complete and uncontaminated sample of the candidate stars. They believe that they have recovered nearly all of the DA WDs hotter than 10,000 K with SDSS spectra.

These stars form the core of our data sample. Eisenstein et al.'s final table lists data on 10,088 WDs. Of these, 7755 are classified as single, nonmagnetic DA's. Kepler et al. (2007) refit the spectra for these stars using the same autofit method and Koester model atmospheres, but with a denser grid which also included models up to log g of 10.0. We use these newer fits in our analysis wherever they differ from Eisenstein et al. Of these 7755 entries, ∼600 are actually duplicate spectra of the same star. For our analysis, we take an average of the values derived from each individual spectrum weighted by the quoted errors. Our final sample contains 7128 single, nonmagnetic DA WDs.

As noted by Kleinman et al. (2004) and others, the surface gravities determined from SDSS spectra show a suspicious upturn below temperatures of about 12,000 K which increases at cooler temperatures, as shown in our Figure 1.

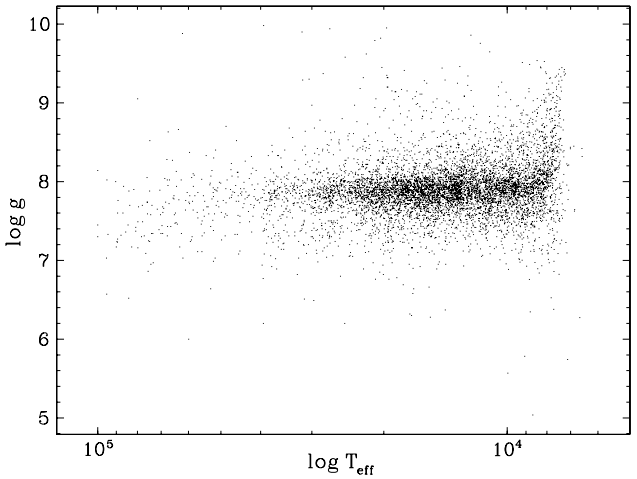

Figure 2. log g versus log $T_{\rm eff}$ with the upturn in log g removed.

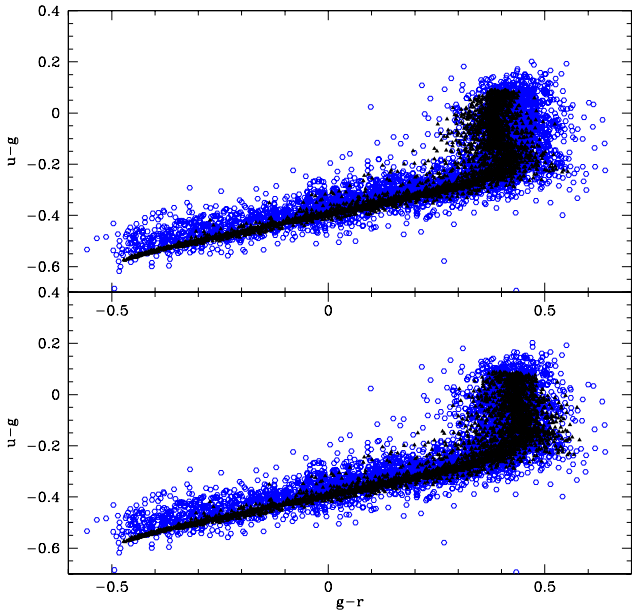

Figure 3. Comparison of the theoretical colors of the SDSS WDs, derived from the atmospheric fits (black triangles), with the observed colors, as measured by the SDSS photometry (open blue circles). In the upper panel, the colors of the model atmospheres do not agree with the observed colors at low temperatures, indicating a problem with the line-fitting for stars cooler than ∼12,500 K. In the lower panel, where the excess log g has been removed, the colors agree much better.

(A color version of this figure is available in the online journal)

A number of separate pieces of evidence argue that this upturn in log g—and thus mass—is an artifact of the models and not a real effect. Not least among these is that no one has yet provided any satisfactory mechanism by which WDs could gain enough mass or shrink enough in radius as they cool to account for the magnitude of the effect. We do expect a slight increase in mass at cooler temperatures because in a galaxy of finite age, the cooler WDs must come from higher mass progenitors. This is the reason for the upward slope of the blue dashed line in Figure 1. However, this effect is clearly small compared to the upturn observed in the actual data.

Furthermore, Engelbrecht & Koester (2007) and Kepler et al. (2007) demonstrated that the masses derived solely from the colors do not show an increase in mass for cooler stars, which indicates that the problem is not physical, but a result of either the line-fitting procedure or the line profiles themselves.

Figure 3 further illustrates the above point. The upper panel shows the colors derived from the synthetic spectra at the values of $T_{\rm eff}$ and log g quoted by Kepler et al. (2007) (i.e., the values in Figure 1) overlaid on the actual SDSS photometry for the same objects. Contrast this with the lower panel, which instead shows the colors derived from the synthetic spectra where the excess log g has been removed (in a manner described below; the resulting values are shown in Figure 2). The colors in the latter figure agree much better with the measured color of the object.

Furthermore, Kepler et al. (2007) found a similar increase in mean mass for the SDSS DB WDs below $T_{\rm eff}$ ∼ 16,000 K. They conclude that since (a) the problem only shows up in the line profiles and not the continuum, and (b) the onset of the effect in both hydrogen (DA) and helium (DB) atmosphere WDs occurs at exactly the effective temperature where the neutral species of the atmospheric element begins to dom-

inate, the problem lies in the treatment of line broadening by neutral particles. This is supported further by the fact that as the species continues to become more neutral (i.e., as the temperature drops), the problem grows worse.

However, more recent model calculations indicate that neutral broadening is not important in the DA WDs at temperatures down to at least 8500 K. Other possible mechanisms to explain the observed upturn in log g include a flawed or incomplete treatment of convection, leading to errors in the temperature structure of the outer layers of the WD models, or the convective mixing of helium from a lower layer in the atmosphere (Bergeron et al. 1990, 1995a). The latter would require a hydrogen layer much thinner than any seismologically determined in a DA so far (Bradley 1998, 2001, 2006).

Until the problem with the model atmospheres is resolved, the best we can do is to empirically remove the log g upturn. For a given $T_{\rm eff}$, we subtract the excess in the measured mean value (as fitted by the red solid lines in Figure 1) over the theoretically expected mean (blue dashed line). Figure 2 shows the resulting values used. In fitting out the upturn this way, we make two implicit assumptions. First, we assume that the excess log g is a function only of $T_{\rm eff}$; if the problem is indeed due to the treatment of neutral particles, we would expect only a small dependence on log g. Second, we assume that the problem affects only the log g determination and not $T_{\rm eff}$. This latter assumption is unlikely to be true, as the two parameters are correlated. In Section 5, we explore more fully the impact of this fitting procedure on the luminosity and mass functions.

3. CONSTRUCTING THE LUMINOSITY AND MASS FUNCTIONS

Since we are dealing with a magnitude-limited sample, the most luminous stars in our sample can be seen at much further distances than the intrinsically fainter stars. We thus expect more of them, proportionally, than we would in a purely volume-limited sample, and must make a correction for the different observing volumes. As shown by Wood & Oswalt (1998) and Geijo et al. (2006), the $1/V_{\rm max}$ method of Schmidt (1968) (described more fully in, e.g., Green (1980); Fleming et al. (1986)) provides an unbiased and reliable characterization of the WD LF.

In the $1/V_{\rm max}$ method, each star's contribution to the total space density is weighted in inverse proportion to the total volume over which it would still be included in the magnitude-limited sample. Since the stars are not spherically distributed, but lie preferentially in the plane of the Galaxy, an additional correction for the scale height of the Galactic disk must be included. For the purposes of comparison with previous work, we adopt a scale height of 250 pc.

To determine the absolute magnitude of each WD, we use the effective temperatures and log g values provided by Kepler et al. (2007)—as corrected in Section 2—and fit each WD with an evolutionary model to determine the mass and radius. For $7.0 < \log g < 9.0$, we use the mixed C/O models of Wood et al. (1995) and Fontaine et al. (2001), as calculated by Bergeron et al. (1995b). For $9.0 < \log g < 10.0$, we use the models of Althaus et al. (2005) with O/Ne cores, including additional sequences for masses larger than 1.3 $M_{\odot}$ calculated specifically for Kepler et al. (2007). Once we know the radius, we can calculate the absolute magnitude in each SDSS band by convolving the synthetic WD atmospheres of Koester (Finley et al. 1997; Koester et al. 2001) with the SDSS filter curves. We apply bolometric corrections from Bergeron et al. (1995b) to determine the bolometric magnitude. For the handful of stars (∼80–100) with log g values outside the range covered by Bergeron's tables, we use a simple linear extrapolation.

We then determine photometric distances to each star from the observed SDSS g magnitude. The SDSS, being concerned mostly with extragalactic objects, reports the total interstellar absorption along each line of sight from the reddening maps of Schlegel et al. (1998). Since the objects in our sample lie within the Galaxy, and most of them within a few hundred parsecs, they are affected by only a fraction of this reddening. Following Harris et al. (2006), we therefore assume that (1) objects within 100 pc are not affected by reddening, (2) objects with Galactic height $|z| > 250$ pc are reddened by the full amount, and (3) the reddening varies linearly between these two values. The distances and reddening are then fit iteratively from the observed and calculated absolute g magnitudes. In practice, the reddening correction makes very little difference to the final LF (typical A_g values range from 0.01 to 0.05).

We calculate error bars on the LF using a Monte Carlo simulation, drawing random deviates in $T_{\rm eff}$, log g, and each band of photometry from Gaussian distributions centered around the measured value. The standard deviations in $T_{\rm eff}$ and log g we use for this scattering are 1.2 times the formal errors quoted in Eisenstein et al. (2006) (their own analysis, based on repeated autofit measurements on duplicate spectra of the same stars, suggests that the formal errors derived by their method are ∼20% too small). The photometry errors come directly from the SDSS database. After scattering the parameters in this way, we recalculate the LF. We then add in quadrature the standard deviation of each LF bin after 200 iterations and the counting error for each bin (the errors for each individual star—taken to be of the order of the star's $1/V_{\rm max}$ statistical weight—summed in quadrature).

At an S/N of 16—the mean for the stars in our sample brighter than $g = 19.5$—formal errors in $T_{\rm eff}$ and log g are of order 1.5%. When propagated through our code, the mean errors in $M_{\rm bol}$ and mass are 0.35 dex and 9% (0.05 $M_{\odot}$), respectively. For the stars brighter than $g = 19.0$ used to compile our mass functions the average S/N is 19.5, leading to errors in $M_{\rm bol}$ and mass of 0.35 dex and 7% (0.04 $M_{\odot}$).

4. COMPLETENESS CORRECTIONS

The chief difficulty we have encountered in deriving our LFs is unraveling the complicated way in which SDSS objects are assigned spectral fibers. The SDSS is foremost a survey of extragalactic objects and rarely targets WDs for follow-up spectroscopy explicitly. Most of the objects in our sample are targeted by some other algorithm. In particular, there is considerable overlap in color between WDs and many QSOs.

A completeness correction could, in theory, be built from "first principles." We know, for each object in the SDSS spectroscopic database, by which algorithm(s) it was targeted (or rejected) for spectroscopy, and by which algorithm it was ultimately assigned a fiber. And for each algorithm, we know which objects were targeted, which were ultimately assigned a fiber, and which, of the targeted objects, turned out to be WDs. However, the selection process is a multivariate function of five apparent magnitudes, and colors in spaces of as many as four dimensions (which vary on the basis of the algorithm), as well as the complex tiling algorithm. We believe such an undertaking to be unnecessary. Instead we have chosen to compare our

sample with the stars used to derive the WD LF of Harris et al. (2006). Given certain assumptions about completeness and contamination in both data sets, we derive a completeness correction as a function of a single color index ($g - i$) and g magnitude.

The Harris et al. (2006) sample comes from photometric data in the SDSS Data Release 3 (DR3). They selected objects by using the reduced proper-motion diagram to separate WDs from more luminous subdwarfs of the same color. Briefly, they used color and proper motion (from USNO-B; Munn et al. 2004) to determine WD candidates from SDSS imaging data. They then fitted candidates with WD model atmosphere colors to determine temperatures and absolute magnitudes, from which they derived photometric distances and—together with proper motion—tangential velocities. In order to minimize contamination, they adopted a tangential velocity cutoff of 30 km s^{-1} and rejected all stars below this limit. The remaining 6000 objects are, with a high and well-defined degree of certainty (∼98–99%), likely to be WDs.

If the database of SDSS spectra were complete, all of these objects would (eventually) have spectra, and all but 1–2% of contaminating objects would be confirmed to be WDs. Furthermore, all of the WDs that did *not* make it into the Harris et al. sample—because they were either missing from the Munn et al. (2004) proper-motion catalog, or had a tangential velocity below 30 km s^{-1}—would also all have spectra. In such a perfect world, of course, no completeness correction would be necessary. However, since the SDSS does not obtain a spectrum of every object in its photometric database, a significant percentage of the objects in Harris et al. will not have spectra, or else will be dropped at some later point by Eisenstein et al. and thus not make it into our spectroscopic sample. Our goal, then, is to look into all of the WDs in the Harris et al. sample that potentially *could* have made it into our sample, and determine which ones in fact did. If we assume that the WDs *not* in Harris et al. follow the same distribution (an assumption we discuss more fully below), then we can take this as a measure of the overall detection probability and invert it to get a completeness correction.

The imaging area of the DR3, from which Harris et al. derive their sample, is not the same as the spectroscopic area in the DR4. Therefore, for the purposes of this comparison, we removed all stars not found in the area of sky common to the two data sets from their respective samples. This left 5340 objects classified as WDs by Harris et al. that could potentially have been recovered by Eisenstein et al. Of these, 2572 were assigned spectral fibers in DR4, and 2346 were ultimately confirmed by Eisenstein et al. to be WDs.

Since we wish to restrict our analysis to single (i.e., nonbinary) DA WDs, we removed all stars classified as DA+M stars in either catalog. Unfortunately, given that the Harris catalog contains no further information as to the type of WD, we were unable to remove the non-DA stars and simply compare what remains with the Eisenstein sample. Instead, we compute the completeness for all of the WDs, under the assumption—explored more fully below—that DA's, as the largest component of the WD population, dominate the selection function.

Figure 4 shows a comparison of the two samples. The open symbols are the complete Harris et al. sample (excluding those, as mentioned above, with $V_{\rm tan} < 30$ km s^{-1}, those not in the region of sky covered by spectroscopy, and the DA+M stars). The gray squares lie outside the cuts in the color–color space

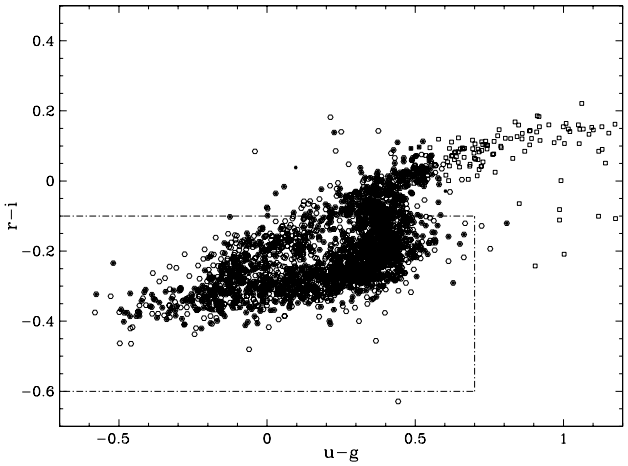

Figure 4. Color–color plot of the WDs in the two samples used to derive our completeness correction. Open symbols are WDs from the Harris et al. (2006) sample that (a) were in the area of sky covered by spectroscopy in DR4, (b) had $V_{\rm tan} \geqslant 30$ km s^{-1}, and (c) were not determined by i- and z-band excess to be WD + main-sequence binaries. The filled circles are the stars for which SDSS obtained spectra and Eisenstein et al. (2006) confirmed to be WDs. The dashed box shows a two-dimensional projection of the QSO targeting algorithm's exclusion region. The open gray squares are the WDs from Harris et al. that lie outside Eisenstein et al.'s color–color cuts. For clarity, only half of the points have been plotted.

imposed by Eisenstein et al. They may have spectra in SDSS, but they were not fit by Eisenstein et al., and therefore will not have made it into our sample. The filled green circles are the stars that *are* in Eisenstein et al. In other words, if the SDSS spectral coverage of WDs were complete, and Eisenstein et al. recovered every WD spectrum in SDSS, then all of the open circles would be filled. The inside of the blue box is the exclusion region for the SDSS's QSO targeting algorithm (Richards et al. 2002), specifically implemented to eliminate WDs from their sample. Note that our sample is more complete for the stars outside this region.

Figure 5 shows the discovery probability as a function of $g-i$ color and g magnitude. Darker areas mean a higher probability of discovery, with black indicating that all the WDs in the Harris et al. sample in the area of color–magnitude space made it into our sample. We have performed a box smoothing to eliminate small scale fluctuations.

There is a drop-off in discovery probability for stars bluer than $g - i \sim -0.2$ at all apparent magnitudes. This corresponds to the red edge of the exclusion region of the QSO targeting algorithm, as noted above. The QSO algorithm is also itself a function of apparent magnitude, which accounts for the general decrease in fainter magnitudes in the red half of the diagram, and the much steeper drop-off between $g \simeq 19$ and $g \simeq 19.5$. The bluer stars ($g - i \lesssim -0.2$), most of which are targeted by the HOT_STANDARD or SERENDIPITY_BLUE algorithms, show the opposite: a slight increase in fainter magnitudes.

To give a better sense of the order of magnitude of our completeness, Figure 6 shows a histogram of the values in Figure 5. For most of the cells that end up in the bins for 0, 1, and 0.5, the Harris et al. sample contains only one or two stars. The mean completeness for the whole sample is ∼51%.

To derive our final completeness correction, we must further consider the incompleteness and contamination in the Harris et al. sample itself. Assuming that the SDSS photometric database is essentially complete down to $g = 19.5$, the incompleteness in Harris et al. comes mainly from two sources:

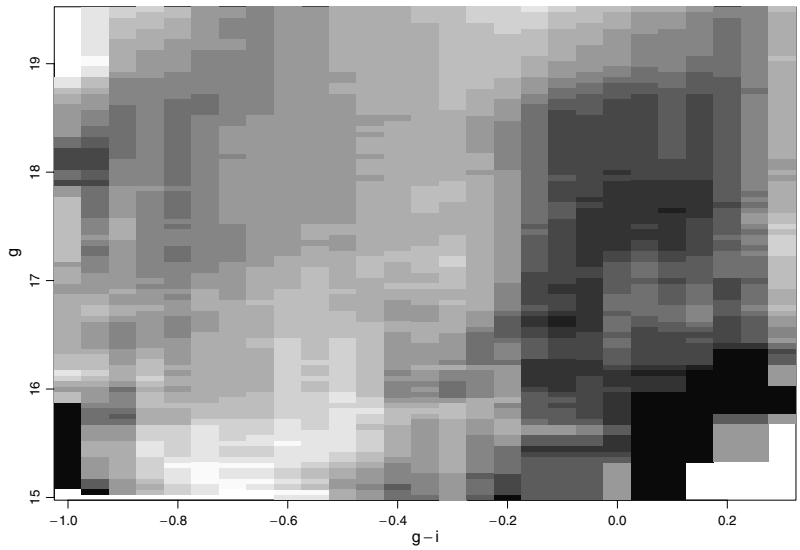

Figure 5. Map of our completeness correction. Darker areas indicate more complete regions of the figure, with black being 100% complete. The overall completeness is of order ∼50%.

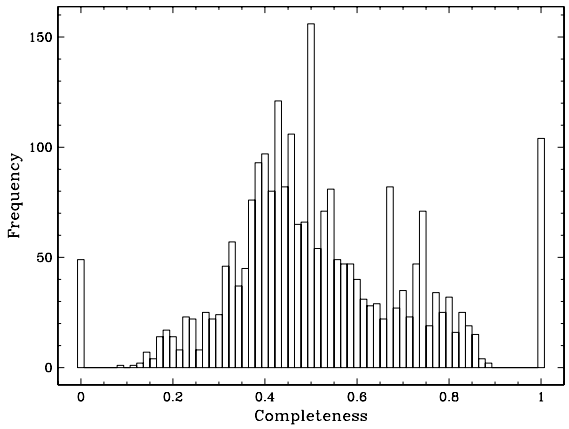

Figure 6. Histogram of the completeness values in Figure 5. Most of the 0, 1, and 0.5 values come from color–magnitude regions in which there are only one or two stars in the Harris et al. sample available for comparison.

(1) the incompleteness in the Munn et al. (2004) proper motion catalog, and (2) the tangential velocity limit of 30 km s^{-1} imposed, which results in some low tangential velocity WDs being dropped from the sample. However, with one negligible exception, none of the criteria used to target objects for spectroscopy in SDSS, nor those used by Eisenstein et al. to select WD candidates, depends explicitly on proper motion or tangential velocity. Thus we assume that the low-velocity stars—dropped from the Harris et al. sample—will be recovered by Eisenstein et al. with the same probability as the high-velocity stars—i.e., the stars in Figure 4.

Contamination poses a somewhat more challenging problem. At first glance, it would seem that the reverse of the above process could be applied, whereby those objects in Harris et al. which did get spectral fibers—but were ultimately rejected as WDs by Eisenstein et al.—could be removed from the sample, and those that did *not* get spectra could be assumed to follow the same distribution. This latter assumption, however, is unlikely to be true. The SDSS gives very low priority to targeting WDs specifically, and we would thus expect a larger fraction of the objects that get spectral fibers to turn out to be contaminating objects (in particular QSOs, of which we found 13 in the Harris et al. sample) than if the fibers were assigned purely randomly. Furthermore, many of the 225 objects that have spectra in DR4 but are not included in the Eisenstein et al. catalog may actually be WDs which Eisenstein et al.'s algorithms dropped for some other reason, e.g., they lie outside the color and magnitude ranges used for initial candidate selection, or there is a problem (low S/N, bad pixels) with the spectrum. Approximately 100 appear to be DC WDs to which the SDSS spectroscopic pipeline assigned erroneous redhifts on the basis of weak noise features. Ultimately, we have chosen to adopt the contamination fraction of Harris et al. (2%) for the whole sample, and have reduced our final completeness correction accordingly. This choice has a negligible effect on the small scale structure of the WD LF in which we are interested.

Finally, we note that the Harris et al. sample has an apparent magnitude limit of $g = 19.5$, whereas the spectroscopic sample contains objects down to $g \simeq 20.5$. Given that the SDSS targeting algorithms are themselves functions of apparent magnitude, our completeness correction is as well. An extrapolation of our discovery probability is problematic in this area, though, because this is exactly the apparent magnitude where the QSO targeting algorithm drops off rapidly. We have decided to impose a magnitude cutoff of $g = 19.5$ in our sample. This reduces our sample by nearly half, with a corresponding increase in counting error. However, since SDSS spectra have a small range of exposure times (45–60 min), fainter apparent magnitude usually translates directly into lower S/N and larger errors in derived parameters.

Figure 7 shows the LFs we derive for different choices of limiting magnitude. We take the generally good agreement between the curves to indicate that our completeness correction is doing its job correctly in the g magnitude direction.

Figure 8 similarly shows the mass functions (MFs) we derive for different choices of limiting magnitude. In the case of the MF, the S/N of the spectra becomes a much bigger factor. As a consequence of the essentially constant exposure times of SDSS spectra, the parameters ($T_{\rm eff}$ and log g) determined from the spectra of fainter objects have larger errors, which causes a larger error in mass. Thus, the MF is broadened when

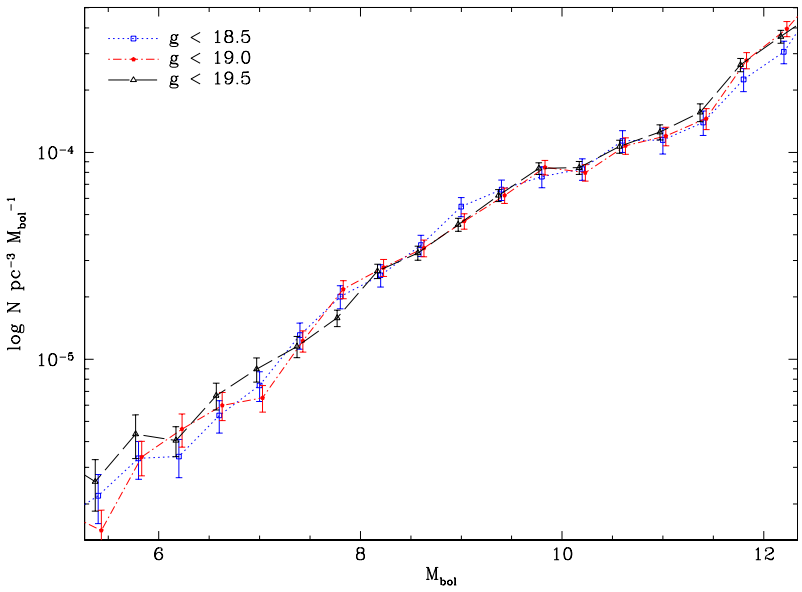

Figure 7. LFs for three different limiting magnitudes. We take the good agreement between the curves to indicate that our completeness correction, and the $1/V_{\rm max}$ correction, are working properly.

(A color version of this figure is available in the online journal)

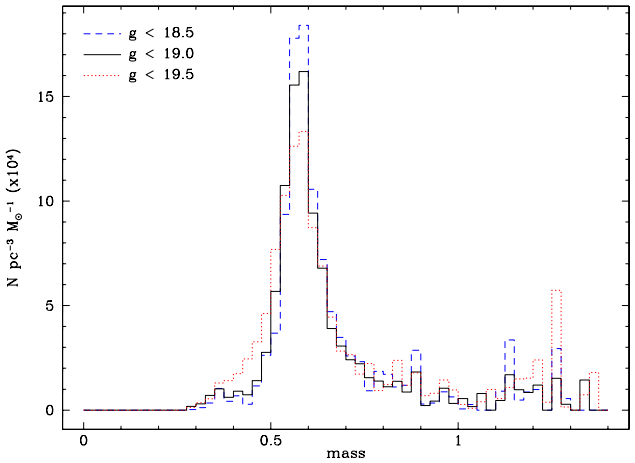

Figure 8. Mass functions for three different limiting magnitudes. Because of the essentially fixed integration time for SDSS spectra, objects with fainter apparent magnitudes generally have lower signal to noise, which translates directly into larger uncertainties in the derived parameters ($T_{\rm eff}$, log g, and mass). Hence, as we include stars with fainter apparent magnitudes, more stars scatter out of the peak, broadening the mass function.

(A color version of this figure is available in the online journal)

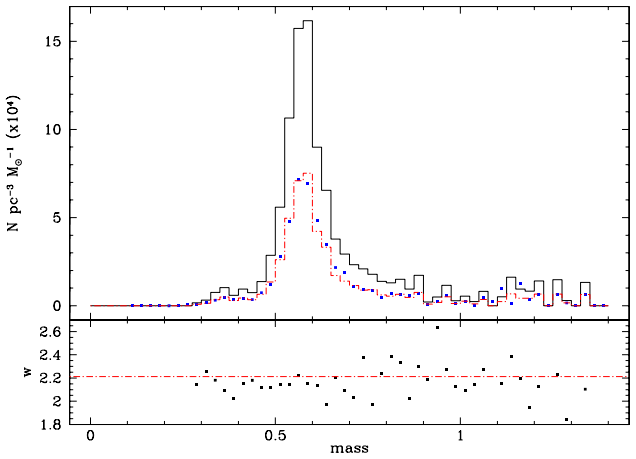

Figure 9. WD mass function for all WDs with $T_{\rm eff} > 12{,}000$ K and $g < 19.0$. The dashed line in the upper panel is the MF corrected only for $1/V_{\rm max}$, without our completeness correction applied. It agrees very well with Kepler et al. (2007—dots). The solid line is with our completeness correction applied, and represents the true local space density of WDs. The bottom panel shows the ratio of our two mass functions—i.e., the cumulative completeness correction for each bin. The small variation indicates that the completeness correction, while changing the overall normalization by roughly a factor of 2.2, has little effect on the shape of the MF.

(A color version of this figure is available in the online journal)

stars with $g > 19.0$ are included. For this reason, Kepler et al. (2007) limited their mass functions to stars with $g \leqslant 19.0$, and we follow their lead for the remaining MFs in the current paper.

5. LUMINOSITY FUNCTIONS, AND DISCUSSION

Figure 9 shows the WD mass function we derive for all stars with $T_{\rm eff} > 12{,}000$ K and $g < 19.0$. The red dashed line is the MF corrected only by $1/V_{\rm max}$—i.e., before we apply our completeness correction. It generally shows good agreement with the MF derived in Kepler et al. (2007) (blue points), not surprising considering we use nearly the same data set and very similar WD models. The small differences are due to our use of slightly different sets of data and models, as well as differing treatment of duplicate spectra, and can largely be considered statistical fluctuations. We refer the interested reader to their paper for a more in-depth analysis of the WD MF.

The solid black line in the upper panel shows our MF after correcting for the completeness of the spectroscopic sample. This curve represents the true local space density of WDs per cubic parsec per $M_\odot$ interval. The bottom panel shows the total weight of each bin above the uncorrected MF—essentially the final completeness correction for each bin. There is little small-scale variation from bin to bin, and our completeness correction

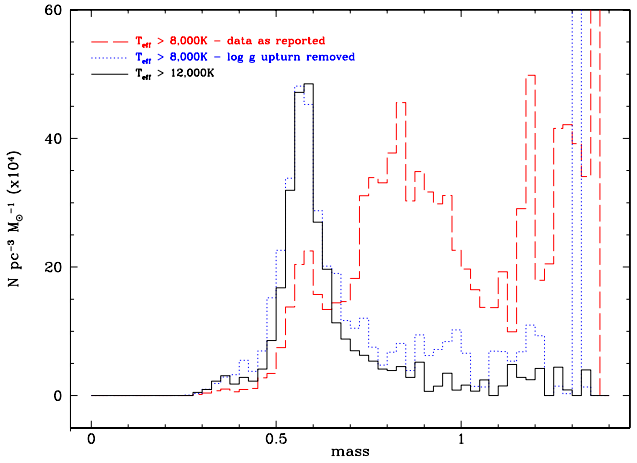

Figure 10. WD MFs for WDs with $T_{\rm eff} > 8000$ K and $g < 19.0$ both with and without the upturn in log g for cooler stars removed. The solid line is the MF from Figure 9 renormalized for comparison purposes.

(A color version of this figure is available in the online journal)

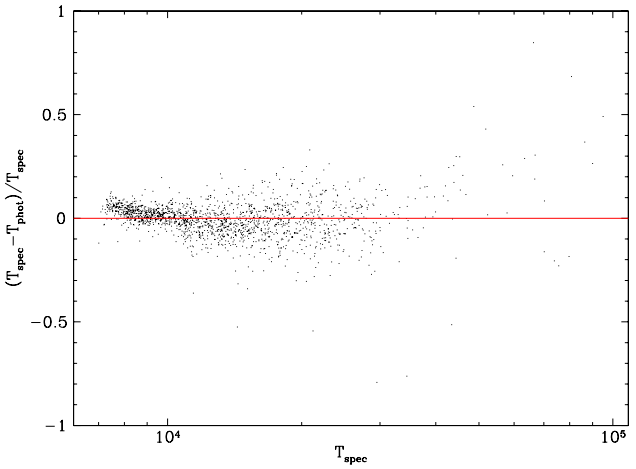

Figure 12. Comparison of the spectrally and photometrically derived temperatures for the WDs common to the Harris et al. (2006) and Eisenstein et al. (2006) samples.

(A color version of this figure is available in the online journal)

mainly has the effect of raising the normalization of the whole MF by a factor of ∼2.2. In other words, the shape of the MF is not strongly affected by the completeness correction.

Figure 10 is the WD MF for all stars down to 8000 K. The dashed red line is for the data as reported by Kepler et al. (2007), the dotted blue line is after our correction for the upturn in log g. The solid black line is the WD MF for only those stars above 12,000 K (i.e., the same as in Figure 9) renormalized to the same scale for comparison purposes. There are more high mass stars in general, and one spuriously large bin, but on the whole, our log g correction recovers a reasonable mass distribution for stars cooler than 12,000 K.

Figure 11 shows the LF we derive for all of the DA stars in our sample down to 7000 K for all stars with $g < 19.5$. Red shows the LF for the data as reported; black shows the LF for the data with the increase in log g at low temperature removed. The process of removing the excess log g pushes stars to lower masses, making them larger and therefore brighter for the same $T_{\rm eff}$. In the range plotted, the black curve contains a total of 3358 WDs, while the red contains 2940.

The lack of agreement between our best LF (black) and the Harris et al. (2006) LF (blue) can be attributed, at least in part, to the differing assumptions used in creating the two LFs. Harris et al. derived their temperatures by fitting Bergeron models to the photometry assuming a log g of 8.0 for every star, a poor assumption for more than 30% of WDs (Liebert et al. 2005; Kepler et al. 2007). The temperatures they derive are systematically different from the spectroscopic temperatures; Figure 12 shows the fractional difference between the spectroscopically and photometrically derived effective temperatures. When we use the photometrically derived temperatures and set log $g = 8.0$, we recover the Harris et al. LF fairly well.

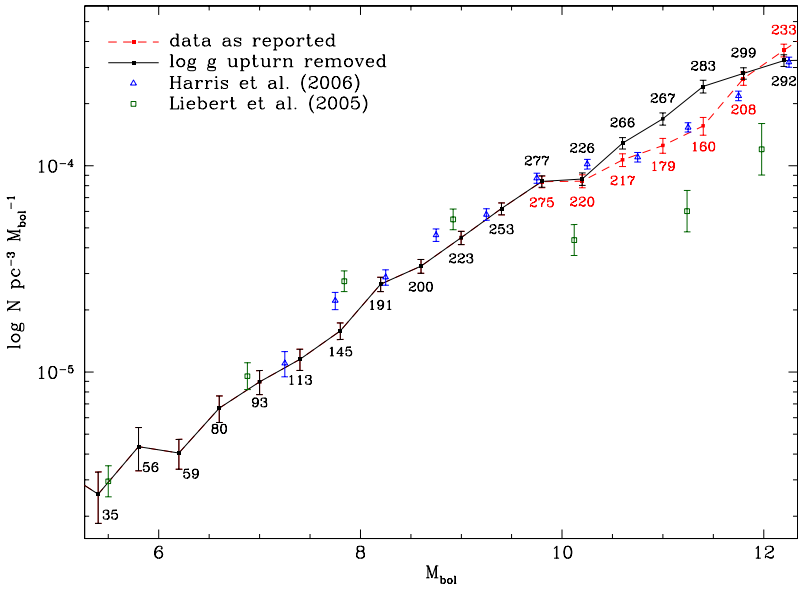

Figure 11. LFs derived in this paper. Removing the log g upturn makes each affected star less massive, and therefore larger and brighter, pushing it to a more leftward $M_{\rm bol}$ bin. The results of Harris et al. (2006) and Liebert et al. (2005) are shown for comparison.

(A color version of this figure is available in the online journal)

It should also be noted that the Harris et al. LF is for WDs of *all* types, whereas ours comprises only the DAs. For each bin in the Harris et al. LF, we have used the full Eisenstein et al. (2006) catalog to determine a rough DA fraction, and reduced the reported Harris et al. LF accordingly. This DA fraction—shown in Table 1—is in generally good agreement with previous works (Fleming et al. 1986), but we have made no attempt to address selection biases in the Eisenstein et al. catalog.

One other source of the discrepancy between our results and those of Harris et al. is due to our assumption that whatever causes the observed upturn in log g in the cooler stars affects only the log g determination and does not alter the spectroscopically derived $T_{\rm eff}$. As the effects of the two parameters on the line profiles are interdependent, this assumption is probably not valid. The curves in Figure 11 suggest that in addition to the excess log g, the temperatures determined by line-fitting for the cooler stars are probably too high. Ultimately, this area of the spectroscopic WD LF will remain uncertain until the problems with the model atmospheres have been resolved.

The LF of Liebert et al. (2005) shown in green in Figure 11 was compiled from a small dataset (348 DA WDs) based on a survey conducted on photographic plates over 20 years ago on a 0.5 m telescope. In addition to low number statistics, the dataset suffers from a very difficult-to-quantify incompleteness on the faint end, which is probably responsible for the lack of agreement below $M_{\rm bol} \sim 9.5$.

6. CONCLUSIONS

Our eventual goal is to take advantage of the tremendous number of WDs spectroscopically observed by the SDSS and studied by Eisenstein et al. (2006) and others to create separate WD LFs for two or more different ranges of mass. This will effectively add a third dimension, currently unexplored, to observational WD LFs.

In order to carry out this analysis, we must fully understand the manner in which WDs were selected to receive spectra in SDSS. By comparing the proper-motion selected sample of Harris et al. (2006) with the spectroscopically determined WDs of Kleinman et al. (2004) and Eisenstein et al. (2006), we have derived a WD selection probability over a range of parameters that includes nearly the entire useful range of $g - i$ color ($-1.0 < g - i < 0.2$) and apparent g magnitude ($15 < g < 19.5$).

We have also presented additional arguments that the observed upturn in log g is an artifact of the model atmosphere line-fitting procedure, or—more likely—a problem with the line profiles themselves. Since it may be some time before this problem is fully understood and addressed, we have implemented a procedure to remove the excess log g empirically and shown that the mass function recovered for the stars cooler than 12,000 K reasonably agrees with the MF for the hotter stars, which in turn agrees well with previous work.

Finally, we have presented the first WD LF for spectroscopically determined WDs in the Fourth Data Release of the SDSS. In addition to addressing the issues of completeness and the observed log g upturn in a more systematic manner than previously attempted, our LF contains the largest sample of spectroscopically determined WDs to date (3,358), more than six times the 531 presented in Hu et al. (2007), and more than an order of magnitude more than the 298 stars included in the LF of Liebert et al. (2005).

We would like to thank Scot Kleinman for providing unpublished fits of the DA WDs; Hugh Harris and Mukremin Kilic for access to the data and code used to derive the Harris et al. (2006) LF, as well as much helpful advice; Barbara Canstanheira, Elizabeth Jeffery, Agnes Kim, Mike Montgomery, Fergal Mullally, and Kurtis Williams for many interesting and insightful discussions.

This material is based on work supported by the National Science Foundation under grant Nos AST 03-07315 and AST 06-07480. This material is partially based upon work supported by the National Aeronautics and Space Administration under Grant No. NAG5-13070 issued through the Office of Space Science.

REFERENCES

Althaus, L. G., García-Berro, E., Isern, J., & Córsico, A. H. 2005, A&A, 441, 689
Althaus, L. G., García-Berro, E., Isern, J., Córsico, A. H., & Rohrmann, R. D. 2007, A&A, 465, 249
Bergeron, P., Liebert, J., & Fulbright, M. S. 1995a, ApJ, 444, 810
Bergeron, P., Wesemael, F., & Beauchamp, A. 1995b, PASP, 107, 1047
Bergeron, P., Wesemael, F., Fontaine, G., & Liebert, J. 1990, ApJ, 351, L21
Blanton, M. R., et al. 2003, AJ, 125, 2276
Bradley, P. A. 1998, ApJS, 116, 307
Bradley, P. A. 2001, ApJ, 552, 326
Bradley, P. A. 2006, Mem. Soc. A Ital., 77, 437
Claver, C. F. 1995, PhD thesis, Univ. of Texas at Austin
Claver, C. F., Liebert, J., Bergeron, P., & Koester, D. 2001, ApJ, 563, 987
Eisenstein, D. J., et al. 2006, ApJS, 167, 40
Engelbrecht, A., & Koester, D. 2007, in Proc. 15th European Workshop on White Dwarfs, Leicester 2006, in press
Finley, D. S., Koester, D., & Basri, G. 1997, ApJ, 488, 375
Fleming, T. A., Liebert, J., & Green, R. F. 1986, ApJ, 308, 176
Fontaine, G., Brassard, P., & Bergeron, P. 2001, PASP, 113, 409
Geijo, E. M., Torres, S., Isern, J., & García-Berro, E. 2006, MNRAS, 369, 1654
Green, R. F. 1980, ApJ, 238, 685
Hansen, B. M. S., et al. 2002, ApJ, 574, L155
Hansen, B. M. S., et al. 2004, ApJS, 155, 551
Hansen, B. M. S., et al. 2007, arXiv:0701738
Harris, H. C., et al. 2003, AJ, 126, 1023
Harris, H. C., et al. 2006, AJ, 131, 571
Hu, Q., Wu, C., & Wu, X.-B. 2007, A&A, 466, 627
Hügelmeyer, S. D., et al. 2006, A&A, 454, 617
Jeffery, E. J., et al. 2007, ApJ, 658, 391
Kepler, S. O., et al. 2007, MNRAS, 375, 1315
Kleinman, S. J., et al. 2004, ApJ, 607, 426
Knox, R. A., Hawkins, M. R. S., & Hambly, N. C. 1999, MNRAS, 306, 736
Koester, D., et al. 2001, A&A, 378, 556
Krzesiński, J., et al. 2004, A&A, 417, 1093
Leggett, S. K., Ruiz, M. T., & Bergeron, P. 1998, ApJ, 497, 294
Liebert, J., Bergeron, P., & Holberg, J. B. 2005, ApJS, 156, 47
Liebert, J., Dahn, C. C., Gresham, M., & Strittmatter, P. A. 1979, ApJ, 233, 226
Liebert, J., Dahn, C. C., & Monet, D. G. 1988, ApJ, 332, 891
Luyten, W. J. 1958, in On the Frequency of White Dwarfs in Space, (Minneapolis, MN: Univ. of Minnesota Obs.)
Munn, J. A., et al. 2004, AJ, 127, 3034
Richards, G. T., et al. 2002, AJ, 123, 2945
Richer, H. B., Fahlman, G. G., Rosvick, J., & Ibata, R. 1998, ApJ, 504, L91
Schlegel, D. J., Finkbeiner, D. P., & Davis, M. 1998, ApJ, 500, 525
Schmidt, M. 1968, ApJ, 151, 393
Stoughton, C., et al. 2002, AJ, 123, 485
von Hippel, T., Gilmore, G., & Jones, D. H. P. 1995, MNRAS, 273, L39
von Hippel, T., et al. 2006, ApJ, 645, 1436
Weidemann, V. 1967, Z. Astrophys., 67, 286
Winget, D. E., et al. 1987, ApJ, 315, L77
Wood, M. A. 1992, ApJ, 386, 539
Wood, M. A. 1995, in Lecture Notes in Physics, White Dwarfs, vol. 443, ed. D. Koester, & K. Werner, (Berlin: Springer), 41
Wood, M. A., & Oswalt, T. D. 1998, ApJ, 497, 870
York, D. G., et al. 2000, AJ, 120, 1579